Modeling the influence of divalent ions on membrane resistance and electric power in reverse electrodialysis

Lucía Gómez-Coma, Víctor M. Ortiz-Martínez, Javier Carmona, Laura Palacio, Pedro Prádanos, Marcos Fallanza, Alfredo Ortiz, Raquel Ibañez, Inmaculada Ortiz

PII: S0376-7388(19)31632-1

DOI: https://doi.org/10.1016/j.memsci.2019.117385

Reference: MEMSCI 117385

To appear in: *Journal of Membrane Science*

Received Date: 31 May 2019

Revised Date: 26 July 2019

Accepted Date: 14 August 2019

Please cite this article as: Lucí. Gómez-Coma, Ví.M. Ortiz-Martínez, J. Carmona, L. Palacio, P. Prádanos, M. Fallanza, A. Ortiz, R. Ibañez, I. Ortiz, Modeling the influence of divalent ions on membrane resistance and electric power in reverse electrodialysis, *Journal of Membrane Science* (2019), doi: https://doi.org/10.1016/j.memsci.2019.117385.

Modeling the influence of divalent ions on membrane resistance and electric power in reverse electrodialysis

Lucía Gómez-Coma[1], Víctor M. Ortiz-Martínez[1], Javier Carmona[2], Laura Palacio[3], Pedro Prádanos[3], Marcos Fallanza[1], Alfredo Ortiz[1], Raquel Ibañez[1], Inmaculada Ortiz[1,*]

[1] Department of Chemical and Biomolecular Engineering. University of Cantabria, Av. Los Castros 46, 39005 Santander, Spain

[2] Department of Applied Physics, Polytechnic School, University of Extremadura, Av. de la Universidad, S/N, 10003 Cáceres

[3] Surface and porous materials Group (SMAP, UA-UVA-CSIC), Department of Applied Physics , Science Faculty, University of Valladolid, 47071 Valladolid, Spain

*corresponding author: ortizi@unican.es

Abstract

The prospects and potential of Reverse Electrodialysis (RED) for energy harvesting from natural streams with salinity gradient demand more in-depth studies to understand and overcome the limitations posed by divalent ions. Power performance is greatly influenced by the ionic resistance displayed by the alternating cation and anion exchange membranes (CEMs and AEMs, respectively) housed in RED stacks, which in turn is determined by the type and concentration of ions and counter-ions in the water streams.

The effects of divalent ions on power output have been experimentally approached in several works by using real or synthetic water. However, the development of comprehensive models including the effect of divalent ions on membrane resistance and power performance under different scenarios is still very scarce. Thus, this work investigates experimentally the effect of ion species on membrane resistance, providing for the first time mathematical correlations useful to predict power performance in RED stacks under a wide range of compositions of salinity gradient solutions. To this end, electrochemical impedance spectroscopy (EIS) measurements have been performed for CEM and AEM commercial membranes in contact with different concentration of NaCl solutions and including different mixtures of divalent ions (Ca^{2+}, Mg^{2+}, SO_4^{2-}). These correlations have been implemented in a previously developed model to determine power outputs as function of ion mixture compositions. Scenarios of general interest for RED practical implementation have been addressed; specifically, solutions with a composition representative of seawater or high salinity brines have been studied as high concentration solutions (HCS) and, on the other hand, typical concentrations of wastewater treatment plant effluents, river water or brackish water from desalination plants were used as low concentration solutions (LCS).

Keywords: Salinity Gradient Energy**;** Reverse Electrodialysis (RED); mathematical model; ion exchange membrane resistance; divalent ions.

1. Introduction

The potential of reverse electrodialysis (RED) in harvesting saline gradient energy has awakened the interest of the scientific community. Since the first report with the principles of the technology by Pattle in 1954 [1], many interesting works have been published, especially in the last two decades [2,3]. Theoretically, a total power of approximately 0.8 kWh could be generated from the flow of 1 m^3 of freshwater into the sea. Potential power generation can amount to nearly 2 TW on the basis of the total freshwater flow of the major rivers worldwide [3]. In general terms, estimated gross global potential of salinity gradient energy (SGE) is higher than 27,000 TWh/year [2].

A RED stack is composed of alternating anion and cation exchange membranes (AEM and CEM, respectively) separated by spacers to create adjacent compartments that are fed with streams of different salinity gradient, named as HCS and LCS [4]. The salinity gradient induces a potential difference over the membranes and the passage of ions promotes electrical current when the HCS is supplied at one side and LCS is driven to the other side of the membranes [5]. Another key component of RED stacks is the electrode couple. At the ends of the stack, an electrode rinse solution (ERS) feeds the electrode compartments to maintain electroneutrality by means of redox reactions, which take place at the cathode and the anode [6]. In laboratory scale plants, an external load connected to the electrodes through an external circuit is used to consume the electrical power generated inside the stack [7].

The presence of divalent ions in water can negatively affect the SGE-RED performance. Previous works have experimentally studied different operational scenarios by operating SGE-RED units fed with real water streams and synthetic waters containing divalent ions [5,8–16]. The most common scenario consists of the use of seawater and river water to provide salinity gradient [5,8,11,12,14,16]. Besides, other authors employed brines and seawater or brackish water as HCS and LCS, respectively [9,10,15,16]. Finally, the performance of fish wastewater as HCS in combination with water coming from an urban wastewater treatment plant (WWTP) as LCS was also assessed [13,16]. The results reported in these works clearly prove that the presence of divalent ions in

RED water streams leads to a reduction in power output and thus their role in RED stacks requires to be specifically addressed. These ions display a strong influence on RED operation and especially on membrane resistance due to their interactions with the fixed charged groups present in the ion exchange membranes [8,9,17–19]. The divalent ions at the highest concentration in these streams usually are magnesium (Mg^{2+}), calcium (Ca^{2+}) and sulphate (SO_4^{2+}). For instance, Avci et al. [9] reported a 7-fold increase in the CEM resistance when instead of 0.5 M pure NaCl a solution composed of 0.3 M $MgCl_2$ and 0.2 M NaCl was employed, due to the presence of magnesium ions. On the other hand, Rijnaarts et al. [8] compared the performance of different types of IEMs, namely heterogeneous membranes (Ralex CMH-PES) and homogenous monovalent-selective and multivalent-permeable membranes (Fuji). For these cases, the membrane resistance increased up to more than 50 % when 10 % of pure NaCl was replaced by $MgCl_2$. This rise in the ionic resistance was higher, as expected, when monovalent-selective membranes (to NaCl) were used.

Despite the availability of previous validated models [6,20–22] for the prediction of the performance of SGE-RED processes under different scenarios, operational variables and stack characteristics, most of these models focus on the study of synthetic sodium chloride solutions without addressing the effects of divalent ions on RED performance, with the exception of the model reported by Hong et al. [23,24]. However, the latter model was only validated with open circuit voltage data. Thus, further efforts are still needed to develop more robust and flexible tools that are capable of predicting RED performance under the presence of mixtures of divalent ions at representative concentrations of real water streams, including natural and industrial waste streams, in order to go one step forward towards the optimization of the technology and its practical implementation.

The aim of this work is to investigate the effect of ion species on membrane resistance and power performance in RED stacks by establishing predictive correlations of membrane resistance as a function of representative compositions of real water streams. For this purpose, electrochemical impedance spectroscopy (EIS) was employed to measure membrane resistance in contact with NaCl solution including mixtures of divalent ions (Ca^{2+}, Mg^{2+}, SO_4^{2}); the membrane resistance was mathematically correlated to the composition of HCS and LCS. Moreover, SGE-RED experiments at laboratory scale were used to validate the mathematical model describing the effect of

divalent ions on RED performance for the recovery of SGE under different scenarios. These scenarios, that have been assessed both in the presence and absence of divalent ions, include (i) typical concentrations of seawater and brine as HCS and (ii) water solutions with concentrations close to 0.02 M NaCl, achievable from wastewater treatment plant streams, river water, brackish water from desalination plants, among other options, as LCS.

2. Experimental and Modelling

2.1 Materials

Solutions were prepared using extra-pure sodium chloride (NaCl, assay >99.5%), provided by Fisher Chemicals, magnesium chloride ($MgCl_2 \cdot 6H_2O$, assay>98%), calcium chloride ($CaCl_2$, assay>95%) both supplied by Panreac, sodium sulphate (Na_2SO_4, assay>99%) delivered by Scharlau and distilled water.

2.2 Membrane Resistance Measurements

The effect of the solution composition on the ionic resistance of Ion Exchange Membranes (IEMs) was studied with the electrochemical impedance spectroscopy (EIS) technique, which is commonly employed to measure membrane resistances [25–28]. EIS measurements were performed by placing the membranes in a nylon cell system (Figure 1). Prior to EIS measurements, membranes were submerged in the different solutions for seven days to ensure impregnation. Membrane samples were then placed between the semi-cells, with a circular shape and 1 cm of diameter (Figure1) and then the compartments were filled with the respective solutions.

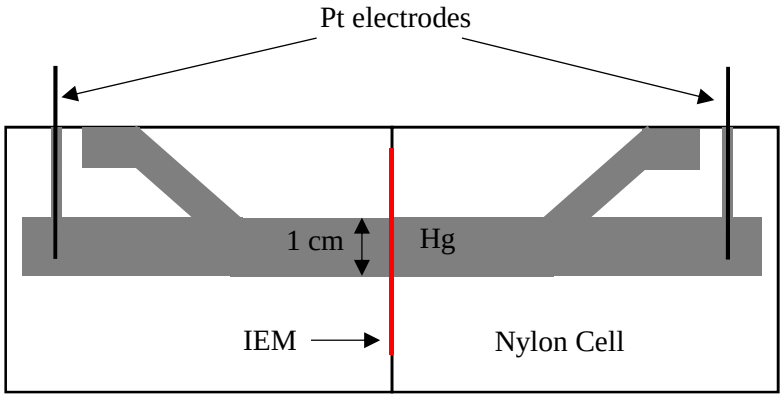

Figure 1. Nylon cell system [29].

Afterwards vacuum was applied to the system in order to remove the air dissolved into the solution while maintaining the solution retained by the membranes. Both semi-cells were filled with mercury displacing the solution excess. Platinum electrodes were dipped in the mercury to close the measuring circuit. The system was isolated from the external electromagnetic field using a stainless steel vessel as Faraday shield and the temperature was kept constant at 297±1 K. Detailed information about this technique has been previously reported [29]. In all cases, the concentration was measured at least 3 times to ensure the measurement reproducibility. NaCl solution concentrations were varied from $6 \cdot 10^{-4}$ M to 1.1 M and both pure NaCl solutions and NaCl solutions with different concentrations of divalent ions were analysed.

EIS measurements were performed using a Solartron 1260 (Ametek, Berwyn, PA, United States) with frequencies from 10 MHz to 10 mHz and under 50 mV. The equipment was controlled by the Solartron Analytical software [29].

2.3 SGE-RED experiments

The SGE experiments were performed using a RED stack with 20 cell pairs formed by AEMs and CEMs of 200 cm^2 (Fumatech®, Germany) and commercial polyethersulfone spacers with a porosity of 82.5% to separate the membranes. Detail of the inner stack configuration can be found in a previous work [22]. The main characteristics of the stack, membranes and spacers are displayed in Table 1.

Table 1. RED stack specifications.

Stack	Cell width (m)	0.063
	Cell length (m)	0.32
	Membrane pairs	20
Membranes	Membrane thickness (m)	$5 \cdot 10^{-5}$
	α AEM permselectivity (0.1/0.5 M)	0.92-0.96
	α CEM permselectivity (0.1/0.5 M)	0.97-0.99
Spacers	Spacers thickness (μm)	270

The electrode rinse solution (ERS) was composed of 0.05 M $K_3Fe(CN)_6$, 0.05 M $K_4Fe(CN)_6$ (Scharlau, purity >99.0%) and 0.25 M NaCl (Fisher Chemicals, assay >99.5%). The ERS solution (adjusted to pH 2-3 with HCl) was continuously recirculated through the electrode compartments.

The stack was continuously fed with the HCS and LCS at constant temperature of 297±1 K. In all cases, the same flow rate was fixed for both streams, equivalent to a Reynolds number of 5.4 (200 mL·min^{-1}). Different concentrations of HCS and LCS were used to validate the model that incorporates the membrane resistance values measured by EIS. As can be seen in Table 2, several compositions of both aqueous NaCl and solutions including divalent ions were used. As HCS, NaCl concentrations close to 0.55 M, corresponding to seawater, and 1 M, the typical composition of sea water desalination brines, were employed. NaCl concentration in LCS was varied from 0.02 M to 0.04 M, which are typical values of wastewater treatment plants effluents; this concentration also represents brackish water from desalination plants, e.g. intermediate streams in two-step reverse osmosis desalination plants. Table 2 gathers the concentration of HCS and LCS analysed in this work.

Table 2. SGE-RED experiment compositions.

Solution	**Scenario**	**Nº**	**NaCl (M)**	**$MgCl_2$ (M)**	**$CaCl_2$ (M)**	**Na_2SO_4 (M)**
LCS	wastewater treatment plant effluents, river water or low salinity brackish water	1	0.02 (synthetic)	0	0	0
		2	0.0172	0.0024	0.0015	0.0014
		3	0.042	0.0011	0.0002	0.0006
HCS	Seawater	4	0.49	0.06	0.011	0.032
	Seawater	5	0.55 (synthetic)	0	0	0
	Brine	6	0.874	0.103	0.02	0.063
	Brine	7	1 (synthetic)	0	0	0
	Brine	8	1	0.114	0.022	0.058

An electronic load (Chroma Systems Solutions 63103A, USA) in the galvanostatic mode was employed to measure the current and voltage of the RED stack. In order to know the maximum power output, polarization tests were performed by varying the current load from 0 A (open circuit voltage, OCV) to 1 A. For each measurement, current load was maintained until the voltage output reached the steady state. Each experiment was repeated at least twice as independent test.

2.4 Model development

A comprehensive model reported in a previous work, implemented in the software Aspen Custom Model V9 (AspenTech), was used to predict the RED stack performance [22]. This model takes into account the equations that describe the phenomena occurring inside the RED stack, establishing the following assumptions: (i) co-current flow distribution, (ii) purely sodium chloride aqueous solutions and, (iii) evaluation of the following parameters at the average conditions between the inlet and the outlet of the cell: cell pair voltage, voltage output, cell resistances, current density and power. The fluxes of H_2O, Na^+ and Cl^- promote a variation in the solutions concentration along the compartments, which are described through mass balance equations. A summary of the main equations employed is detailed below.

The cell pair voltage is determined by the Nernst equation:

$$E_{cell}(x) = \alpha_{CEM} \cdot \frac{R \cdot T}{F} \cdot \left[\frac{1}{z_i} ln\left(\frac{\gamma_{HC}^{Na^+}(x) \cdot C_{HC}^{Na^+}(x)}{\gamma_{LC}^{Na^+}(x) \cdot C_{LC}^{Na^+}(x)}\right)\right] + \alpha_{AEM} \cdot \frac{R \cdot T}{F} \cdot \left[\frac{1}{z_{ion}} ln\left(\frac{\gamma_{HC}^{Cl^-}(x) \cdot C_{HC}^{Cl^-}(x)}{\gamma_{LC}^{Cl^-}(x) \cdot C_{LC}^{Cl^-}(x)}\right)\right] \quad (1)$$

where α_{CEM} and α_{AEM} are the permselectivity of IEMs, F is the Faraday's constant (C mol^{-1}), R is the Universal gas constant (8.314 $J \cdot mol^{-1} \cdot K^{-1}$), T is the temperature (K), C is the ion concentration ($mol \cdot m^{-3}$), z is the valence and γ is the activity coefficient.

The voltage output (E) can be calculated as the theoretical voltage from all the stack cell pairs minus the voltage drop due to the total internal resistance in the stack (R_{stack}).

$$E = \sum E_{cell} - j \cdot R_{stack} \quad (2)$$

where $\sum E_{cell}$ is the sum of all the cell pair voltages (V), j is the electrical current density ($A \cdot m^{-2}$) and R_{stack} is the sum of all the cell pair internal resistances ($\Omega \cdot m^2$). These internal resistances comprise two main components of ohmic and non-ohmic nature, respectively: (i) ohmic resistances composed of the membrane and compartment resistances and (ii) non-ohmic resistances formed by $R_{\Delta C}$, which is caused by the streamwise concentration change, and the boundary layer resistance, R_{BL}.

Finally, gross power, P (W), is calculated as the product of the output voltage and the electric current (A), as shown in equation 3.

$$P = E \cdot I \tag{3}$$

For the model solution, only Na^+ composition was considered for the inlet stream concentration, and the effect of the presence of divalent ions was considered through the resistance of the membrane using empirical correlations proposed through experimental tests. Empirical correlations were obtained for the cationic and anionic membranes, respectively, for LCS and HCS. All correlations include two main parts, the first one that considers the Na^+ or Cl^- contribution and the second part that considers the contribution of divalent ions.

3. Results and discussion

In this section, membrane resistances measured by electrical impedance spectroscopy (EIS) and the outcomes of SGP-RED experiments are presented; furthermore, the validation of the proposed model, which includes the effect of divalent ions on membrane resistances, is also displayed.

Membrane resistances were determined after being in contact with solutions of NaCl and divalent ions, Mg^{2+}, Ca^{2+} and SO_4^{2-}, at the concentrations of HCS and LCS collected in Table 2.

3.1 Membranes resistances

The resistance of the membranes was firstly assessed using pure NaCl solutions. For this purpose, four different solutions with concentrations ranging from $6 \cdot 10^{-4}$ M to 1 M were prepared. Figure 2 shows the respective resistance values determined for the CEMs and AEMs.

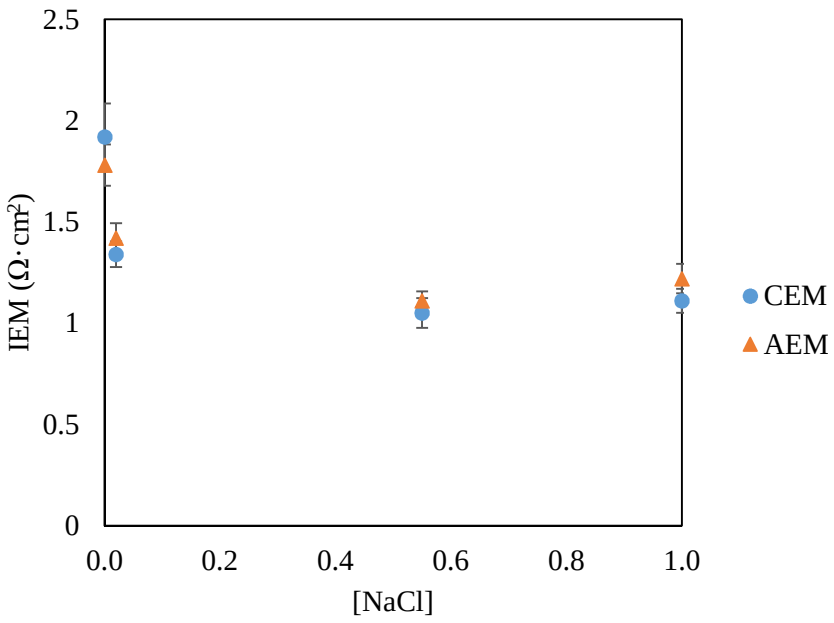

Figure 2. Membrane resistance values measured using pure NaCl at 297±1 K.

As can be seen in Table 3, the CEM resistance sharply decreases with increasing NaCl concentration from $6 \cdot 10^{-4}$ M to 0.02 M, with a total reduction of 30 %. In the case of the AEM, the observed decrease is lower (20 %) for this range of concentration. Besides, for both membrane types, the membrane resistance continues decreasing as the concentration rises up to 0.55 M, but it tends to stabilise in the range from 0.55 M to 1 M, which is in agreement with previously reported works [17,30]. An empirical correlation for the membrane resistance of each IEM type is proposed as a function of sodium and chloride mole fractions, respectively. Eq. 4.a and 4.b show the correlations for CEMs and AEMs as function of the molar fraction (X) with regression coefficients R^2>0.99 in both cases.

$$R_{membrane} CEM\ (NaCl) = \frac{0.686}{X_{Na^+}^{0.089}} \qquad (4.a)$$

$$R_{membrane} AEM\ (NaCl) = \frac{0.809}{X_{Cl^-}^{0.069}} \qquad (4.b)$$

Membrane resistances with NaCl and different concentrations of divalent ions were also determined. Table 3 shows the concentration of the solutions together with the measured values of membrane resistance for the CEM ($\Omega \cdot cm^2$).

According to the results, two general trends for membrane resistance were observed as a function of NaCl concentration when divalent ions were added. On one hand, the addition of divalent ions promotes a strong increase in the CEM resistance for NaCl concentrations below 0.043 M (Table 3). On the other hand, this rise is less pronounced when NaCl concentrations are higher than 0.5 M (corresponding to high salinity waters). This fact is also in good agreement with the results reported in previous works [31,32].

Table 3. CEM resistance measured using pure NaCl and NaCl solutions containing divalent cations at 297±1 K.

NaCl (M)	$MgCl_2$ (M)	$CaCl_2$ (M)	CEM resistance ($\Omega \cdot cm^2$)
$6 \cdot 10^{-4}$	0	0	1.92
0.02	0	0	1.34
0.02	$1.0 \cdot 10^{-4}$	0	2.36
0.02	$1.0 \cdot 10^{-3}$	0	4.87
0.02	0	$1.0 \cdot 10^{-4}$	2.04
0.02	0	$1.0 \cdot 10^{-3}$	4.40
0.02	0	$5.0 \cdot 10^{-3}$	5.81
$6 \cdot 10^{-4}$	$2.86 \cdot 10^{-4}$	$1.19 \cdot 10^{-3}$	5.47
0.02	$2.4 \cdot 10^{-3}$	$1.5 \cdot 10^{-3}$	5.46
0.043	$1.1 \cdot 10^{-3}$	$2.0 \cdot 10^{-4}$	3.56
0.55	0	0	1.05
1	0	0	1.11
1	0.05	0	2.14
1	0.1	0	2.53
1	0.2	0	2.72
1	0	0.01	1.93
1	0	0.02	2.03
1	0	0.1	2.91

Furthermore, the individual effects of the addition of Mg^{2+} or Ca^{2+} ions to CEM resistance are quite similar. In both cases, when the divalent ion concentration (Mg^{2+} or Ca^{2+}, respectively) was varied from 10^{-4} M to 10^{-3} M, the membrane resistance experimented a significant increase by more than doubling its value. In particular, the

CEM resistances rose from 2.36 Ω·cm^2 (Mg^{2+}) and 2.04 Ω·cm^2 (Ca^{2+}) to 4.87 Ω·cm^2 (Mg^{2+}) and 4.40 Ω·cm^2 (Ca^{2+}), respectively. It is worth noting that divalent cations display a notable effect on the CEM membrane resistance even at very low concentration. For higher NaCl concentrations, the increase in membrane resistance due to the addition of divalent ions is lower. When 0.1 M of these divalent ions were added to 1 M NaCl, CEM resistances were 2.53 Ω·cm^2 (Mg^{2+}) and 2.91 Ω·cm^2 (Ca^{2+}), while the resistance corresponding to 1 M NaCl was 1.11 Ω·cm^2. According to these results, two correlations for CEM resistance are proposed taking into account the presence of these divalent cations within the two previously differentiated NaCl concentration ranges, which would represent LCS and HCS respectively. These correlations are presented in eq. 5 and offer regression coefficients of R^2>0.93 (Eq. 5a) and R^2>0.95 (Eq. 5b).

$$6 \cdot 10^{-4} M \leq NaCl\ M \leq 0.043\ M$$

$$R_{membrame}CEM = \frac{0.686}{X_{Na^+}^{0.089}} + \frac{359}{X_{divalent\ cations}^{-0.456}} \qquad (Eq.\ 5a)$$

$$0.5\ M \leq NaCl\ M \leq 1.1\ M$$

$$R_{membrane}CEM = \frac{0.686}{X_{Na^+}^{0.089}} + \frac{5.51}{X_{divalent\ cations}^{-0.209}} \qquad (Eq.\ 5b)$$

In the case of the AEM resistances (Table 4), the trend is the same as that found for CEMs. Two correlations, one for the lowest NaCl concentration range ($3 \cdot 10^{-4}$ M ≤ NaCl M ≤ 0.05 M) and a second one for the highest NaCl values (0.6 M ≤ NaCl M ≤ 1.3 M) are proposed in Eq. 6 with correlation coefficients of R^2>0.94 and R^2>0.96, respectively. However, in this case, the contribution of the SO_4^{2-} ions to the total membrane resistance was lower than that displayed by the cationic divalent ions on the CEM. When $5 \cdot 10^{-3}$ M of SO_4^{2-} was added to a solution of 0.02 M NaCl, the AEM resistance value increased from 1.42 Ω·cm^2 to 2.04 Ω·cm^2. In contrast, when the same concentration of Ca^{2+} was added, the CEM resistance increased from 1.34 Ω·cm^2 to 5.81 Ω·cm^2. Moreover, the addition of different quantities of SO_4^{2-} to 1 M NaCl (1.22 Ω·cm^2) had negligible influence on the AEM resistance (Table 4).

$$3 \cdot 10^{-4} M \leq NaCl\ M \leq 0.05\ M$$

$$R_{membrane}AEM = \frac{0.809}{X_{Cl^-}^{0.069}} + \frac{2.261}{X_{divalent\ anions}^{-0.131}} \qquad (Eq.6a)$$

$$0.6\ M \leq NaCl\ M \leq 1.3\ M$$

$$R_{membrane}AEM = \frac{0.809}{X_{Cl^-}^{0.069}} + \frac{0.731}{X_{divalent\ anions}^{-0.181}} \qquad (Eq.6b)$$

Table 4. AEM resistances measured using pure NaCl and divalent anions.

NaCl (M)	Na_2SO_4 (M)	AEM resistance ($\Omega \cdot cm^2$)
$6 \cdot 10^{-4}$	0	1.78
0.02	0	1.42
0.02	$1.0 \cdot 10^{-4}$	1.79
0.02	$1.0 \cdot 10^{-3}$	1.99
0.02	$5.0 \cdot 10^{-3}$	2.04
0.55	0	1.11
1	0	1.22
1	0.01	1.23
1	0.06	1.27
1	0.1	1.31

3.2 SGE-RED experiments

In this section, the effect of divalent ions in terms of gross power is studied taking into account the representative concentrations of real scenarios. For this purpose, several experiments were performed with pure NaCl and divalent ions at representative concentrations of real water streams suitable for power generation as shown in Table 2.

The correlations obtained to estimate the resistance of the CEM and AEM were implemented in the mathematical model previously developed to predict the power output accounting for the effect of the divalent ions on RED performance. Experimental data were compared to simulated results under different scenarios to validate the model proposed including the membrane resistance correlations. In all cases, the Reynolds

number was 5.4, which is equivalent to a linear flow velocity of 1.2 cm·s^{-1} and the temperature was maintained constant at 297±1 K.

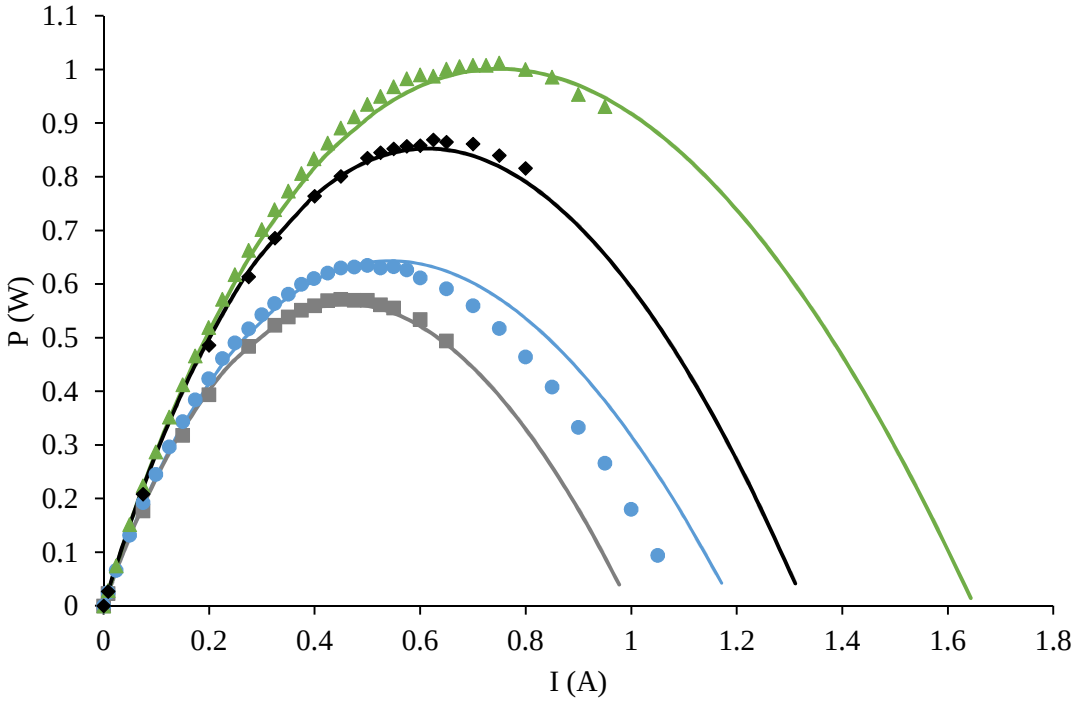

Figure 3. Power curves for (i) Pure NaCl: ▲HCS = 1 M and a LCS = 0.02 M, ● HCS = 0.55 M and LCS = 0.02 M; (ii) NaCl and divalent ions: ◆ HCS (Na^+) = 1 M and LCS (Na^+) = 0.02 M, ■ HCS (Na^+) = 0.55 M and LCS (Na^+) = 0.02 M. Experimental (points) and simulated (lines). T^a = 297±1 K.

Figure 3 shows the gross power achieved for the combinations 1-0.02 M and 0.55-0.02 M, in the presence and absence of divalent ions. 1 M corresponds to brine concentration and, on the other hand, 0.55 M is the typical salt concentration for seawater. As observed, experimental data are in good concordance with the simulated results when using the empirical correlations proposed for membrane resistances. When 1 M pure NaCl was used as HCS, the maximum power achieved was 1 W, equivalent to a power density of 1.25 W·m^{-2}, and the limiting current was as high as 1.7 A. On the other hand, when pure NaCl was used at concentrations of HCS=0.55 M, a maximum gross power density of 0.63 W (0.8 W·m^{-2}) was reached. Comparing the maximum power outputs obtained for HCS at 1 M pure NaCl and 0.5 M (for a fixed LCS of 0.02 M), it is worth noting that there is not a linear relationship between the HCS concentration and the maximum power obtained. Thus, doubling the NaCl concentration in the HCS does not lead to double the power due to the effect of the membrane resistance values corresponding to each concentration.

In order to analyse the effect of the presence of divalent ions on the stack performance, experiments were carried out by adding the divalent ions Mg^{2+}, Ca^{2+} and SO_4^{2-} at the representative concentrations of the scenarios included in Table 2 for HCS and LCS. Furthermore, simulations were run taking into account the correlations proposed in section 3.1 to calculate membrane resistances.

Figure 3 also shows the results obtained for the scenarios corresponding to the combination of HCS=0.55 M (seawater) with a LCS=0.02 M (Table 2, LCS=Nº 2 and HCS=Nº 4) as well as the combination of HCS=1 M (brines) with LCS = 0.02 M (Table 2, LCS=Nº 2 and HCS=Nº 6). In the first case, a gross power density of 0.58 W was reached working with divalent ions, equivavent to a reduction of 8.6 % when pure NaCl was used. On the other hand, when the combination HCS (Na^+) = 1 M and LCS (Na^+) = 0.02 was studied, a maximum gross power density of 1.075 $W \cdot m^2$ was achieved equivalent to a reduction of 16.3 % with regard to the use of pure NaCl. However, these maximum gross power density values are higher than the values reported by previous works that compare synthetic and real waters. Tedesco et al (2016) described a significant decrease down to 40 % in gross power density with respect to theoretical power density when the feed solutions were switched from synthetic brackish water/brine (pure NaCl) to real natural solutions [15]. For its part, Kingsbury et al. (2017) reported reductions of 43 % and 32 % when seawater was used in combination with brackish water and river water respectively [16] .

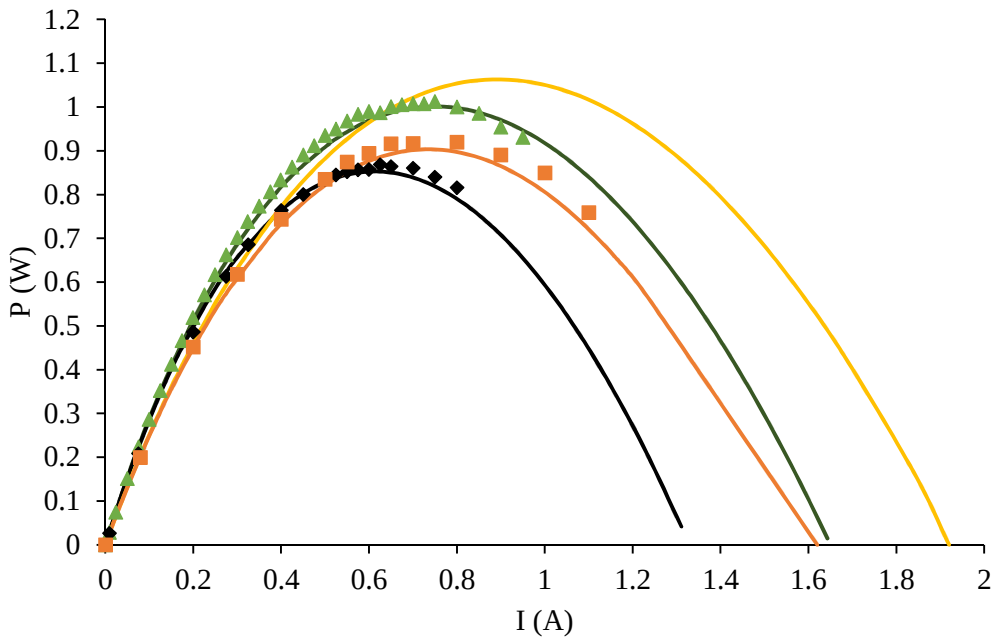

Figure 4. Power curves for (i) pure NaCl: ▲ HCS = 1 M and LCS = 0.02 M, ━ HCS = 1.1 M and LCS = 0.043 M; (ii) NaCl and divalent ions: ■ HCS (Na^+) = 1.1 M and LCS (Na^+) = 0.043 M, ◆ HCS (Na^+) = 1 M and LCS (Na^+) = 0.02 M. Experimental (points) and simulated (lines). T^a = 297±1 K.

Figure 4 displays both experimental (points) and simulated (lines) results for the combination of the scenarios related to high salinity brines as HCS and WWTP, river water or intermediate brackish waters of desalination plants as LCS, with the corresponding concentrations of divalent ions. For comparison purposes, Figure 4 also includes the power curve for pure NaCl (in the absence of divalent ions). The simulated results obtained were in good agreement with the experimental data, confirming that the presence of divalent ions reduces the maximum gross power due to the consequent increase in membrane resistance.

Considering the scenarios nº 3 and nº 8 as LCS and HCS, respectively, both in the presence and in the absence of divalent ions, the same trends were observed as those found for the combination 1-0.02 M. Once again the simulated results employing the values of resistance estimated for the membranes with the implementation of the correlations obtained in section 3.1 fit well to experimental data. For this scenario, the values of membrane resistance for CEMs and AEMs are lower in comparison to those found for the previous combination of 1M (HC) - 0.02 M (LC), but the increase in power output accounts for only 7 % (1.15 $W \cdot m^2$). This is because the ratio between HCS and LCS (salinity gradient) is reduced by half, which has a negative effect on

power performance in comparison, and it hinders the improvement expected by the reduction of membrane resistance.

According to the results presented, divalent ions such as Mg^{2+}, Ca^{2+} and SO_4^{2-} have a negative effect on the maximum power output due to the increase in membrane resistance. And, this effect can be included in the prediction of RED power performance through proper correlations between the concentration of divalent ions and the corresponding AEM and CEM resistances. For the scenarios analysed, which comprise real water stream concentrations, the maximum decrease in power output due to the presence of divalent ions was 16.3 %. Although this decrease is relevant, it can be considered acceptable for the deployment and scale-up of the technology.

The block diagram presented in Figure 5 summarizes the procedure followed in this work and the variables required to model RED performance in terms of gross power. IEMs play a key role on RED technology and therefore both CEM and AEM resistances need to be quantified by the EIS technique taking into account ion composition. In addition, the main characteristics of the RED system, thickness and porosity of spacers, IEM permselectivity and experimental conditions (flowrate, temperature and composition) have to be considered for a comprehensive modelling approach.

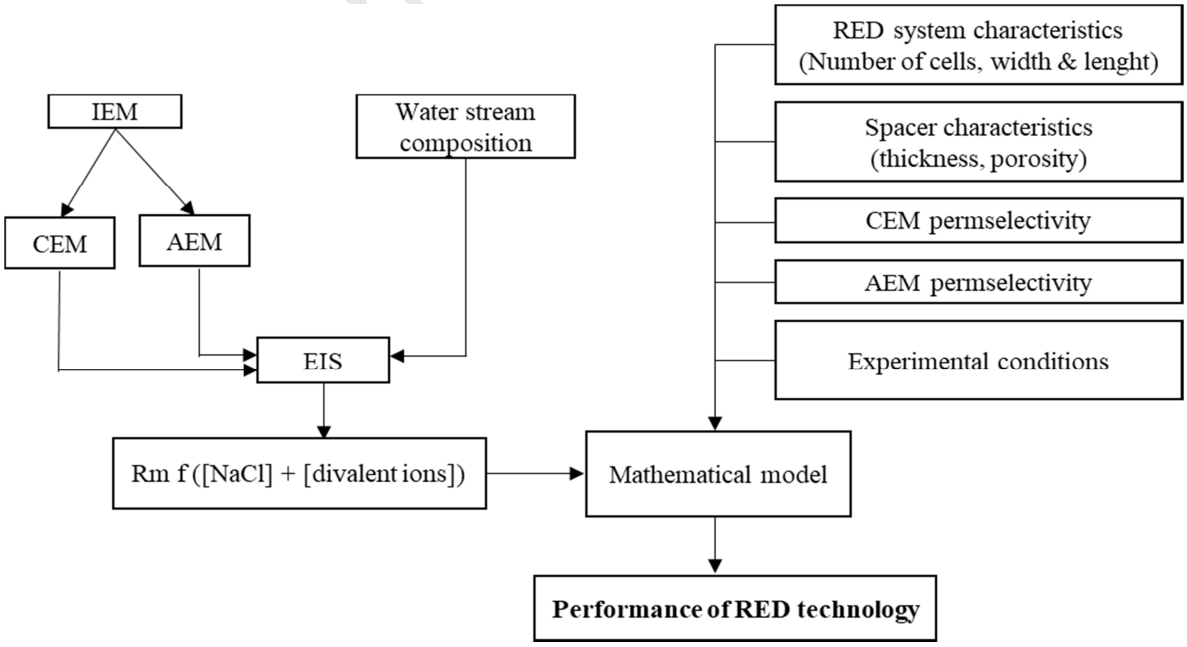

Figure 5. Block diagram of RED power prediction.

4. Conclusions.

Reverse Electrodialysis (RED) offers great potential for harnessing the energy contained in salinity gradient. The development of comprehensive mathematical tools for the prediction of power peformance under real scenarios is essential for the design and optimization of this technology. Due to its importance, the effect of divalent ions on membrane resistance needs to be specifically approached. For this purpose, mathematical correlations for the resistance of commercial ion exchange membranes as a function of both pure NaCl and divalent ions, which pose negative effects on RED performance, have been proposed and implemented in a previously developed model to accurately predict power output under different scenarios. The effect of the main divalent ions present in water streams used in RED, i.e. $Ca^{2+,}$ $Mg^{2+,}$ SO_4^{2-}, has been determined experimentally in terms of CEM and AEM resistances leading to predictive correlations of membrane resistance as function of ion concentrations. These correlations have been integrated in a mathematical model in order to predict the power output under a wide range of HCS and LCS scenarios. Model validation was accomplished by experimental data obtained in a RED stack using synthetic solutions at representative concentrations of NaCl and the above mentioned divalent ions. The results showed that the presence of divalent ions leads to a maximum reduction of 16.3 % in terms of maximum power output in comparison to scenarios that only employ pure NaCl, for the combination of HCS (Na^+) = 1 M and LCS (Na^+) = 0.02 M. This reduction is explained by the increase in the resistance of the cation and anion exchange membranes employed in RED stacks. Thus, a robust mathematical tool, that considers the effect of divalent ions on IEMs resistances, has been developed in order to study the power yield when using real water streams in RED systems.

Acknowledgements

The authors want to acknowledge financial support from the Community of Cantabria - Regional Plan through the project: Gradisal “RM16-XX-046-SODERCAN/FEDER”, and to the projects funded by the Spanish Ministry of Economy and Competitiveness CTQ2015-66078-R, and CTM2017-87850-R. V.M. Ortiz-Martínez is supported by the Spanish Ministry of Science, Innovation and Universities (grant ‘Juan de la Cierva-Formación’ ref. FJCI-2017-32404).

References

[1] R.E. Pattle, Production of Electric Power by mixing Fresh and Salt Water in the Hydroelectric Pile, Nature. 174 (1954) 660–660. doi:10.1038/174660a0.

[2] R.A. Tufa, S. Pawlowski, J. Veerman, K. Bouzek, E. Fontananova, G. di Profio, S. Velizarov, J. Goulão Crespo, K. Nijmeijer, E. Curcio, Progress and prospects in reverse electrodialysis for salinity gradient energy conversion and storage, Appl. Energy. 225 (2018) 290–331. doi:10.1016/j.apenergy.2018.04.111.

[3] Y. Mei, C.Y. Tang, Recent developments and future perspectives of reverse electrodialysis technology: A review, Desalination. 425 (2017) 156–174. doi:10.1016/j.desal.2017.10.021.

[4] E. Farrell, M.I. Hassan, R.A. Tufa, A. Tuomiranta, A.H. Avci, A. Politano, E. Curcio, H.A. Arafat, Reverse electrodialysis powered greenhouse concept for water- and energy-self-sufficient agriculture, Appl. Energy. 187 (2017) 390–409. doi:10.1016/j.apenergy.2016.11.069.

[5] D.A. Vermaas, J. Veerman, M. Saakes, K. Nijmeijer, Influence of multivalent ions on renewable energy generation in reverse electrodialysis, Energy Environ. Sci. 7 (2014) 1434–1445. doi:10.1039/C3EE43501F.

[6] M. Tedesco, A. Cipollina, A. Tamburini, W. van Baak, G. Micale, Modelling the Reverse ElectroDialysis process with seawater and concentrated brines, Desalin. Water Treat. 49 (2012) 404–424. doi:10.1080/19443994.2012.699355.

[7] J. Veerman, M. Saakes, S.J. Metz, G.J. Harmsen, Reverse electrodialysis: Evaluation of suitable electrode systems, J. Appl. Electrochem. 40 (2010) 1461–1474. doi:10.1007/s10800-010-0124-8.

[8] T. Rijnaarts, E. Huerta, W. van Baak, K. Nijmeijer, Effect of Divalent Cations on RED Performance and Cation Exchange Membrane Selection to Enhance Power Densities, Environ. Sci. Technol. (2017) acs.est.7b03858. doi:10.1021/acs.est.7b03858.

[9] A.H. Avci, P. Sarkar, R.A. Tufa, D. Messana, P. Argurio, E. Fontananova, G. Di

Profio, E. Curcio, Effect of Mg 2+ ions on energy generation by Reverse Electrodialysis, J. Memb. Sci. 520 (2016) 499–506. doi:10.1016/j.memsci.2016.08.007.

[10] A.H. Avci, P. Sarkar, D. Messana, E. Fontananova, G. Di Profio, E. Curcio, Effect of MgCl2 on Energy Generation by Reverse Electrodialysis, in: Int. Conf. Nanotechnol. BASED Innov. Appl. Environ., 2016: pp. 361–366. doi:10.3303/CET1647061.

[11] D.A. Vermaas, D. Kunteng, J. Veerman, M. Saakes, K. Nijmeijer, Periodic feedwater reversal and air sparging as antifouling strategies in reverse electrodialysis, Environ. Sci. Technol. 48 (2014) 3065–3073. doi:10.1021/es4045456.

[12] J.W. Post, H.V.M. Hamelers, C.J.N. Buisman, Influence of multivalent ions on power production from mixing salt and fresh water with a reverse electrodialysis system, J. Memb. Sci. 330 (2009) 65–72. doi:10.1016/J.MEMSCI.2008.12.042.

[13] J. Luque Di Salvo, A. Cosenza, A. Tamburini, G. Micale, A. Cipollina, Long-run operation of a reverse electrodialysis system fed with wastewaters, J. Environ. Manage. 217 (2018) 871–887. doi:10.1016/j.jenvman.2018.03.110.

[14] J. Moreno, V. Díez, M. Saakes, K. Nijmeijer, Mitigation of the effects of multivalent ion transport in reverse electrodialysis, J. Memb. Sci. 550 (2018) 155–162. doi:10.1016/j.memsci.2017.12.069.

[15] M. Tedesco, C. Scalici, D. Vaccari, A. Cipollina, A. Tamburini, G. Micale, Performance of the first reverse electrodialysis pilot plant for power production from saline waters and concentrated brines, J. Memb. Sci. 500 (2016) 33–45. doi:10.1016/j.memsci.2015.10.057.

[16] R.S. Kingsbury, F. Liu, S. Zhu, C. Boggs, M.D. Armstrong, D.F. Call, O. Coronell, Impact of natural organic matter and inorganic solutes on energy recovery from five real salinity gradients using reverse electrodialysis, J. Memb. Sci. 541 (2017) 621–632. doi:10.1016/j.memsci.2017.07.038.

[17] A.H. Galama, D.A. Vermaas, J. Veerman, M. Saakes, H.H.M. Rijnaarts, J.W.

Post, K. Nijmeijer, Membrane resistance: The effect of salinity gradients over a cation exchange membrane, J. Memb. Sci. 467 (2014) 279–291. doi:10.1016/j.memsci.2014.05.046.

[18] R.A. Tufa, E. Curcio, W. van Baak, J. Veerman, S. Grasman, E. Fontananova, G. Di Profio, Potential of brackish water and brine for energy generation by salinity gradient power-reverse electrodialysis (SGP-RE), RSC Adv. 4 (2014) 42617–42623. doi:10.1039/C4RA05968A.

[19] Y. Oh, Y. Jeong, S.J. Han, C.S. Kim, H. Kim, J.H. Han, K.S. Hwang, N. Jeong, J.S. Park, S. Chae, Effects of Divalent Cations on Electrical Membrane Resistance in Reverse Electrodialysis for Salinity Power Generation, Ind. Eng. Chem. Res. 57 (2018) 15803–15810. doi:10.1021/acs.iecr.8b03513.

[20] M. Tedesco, A. Cipollina, A. Tamburini, I.D.L. Bogle, G. Micale, A simulation tool for analysis and design of reverse electrodialysis using concentrated brines, Chem. Eng. Res. Des. 93 (2015) 441–456. doi:10.1016/j.cherd.2014.05.009.

[21] M. Tedesco, H.V.M. Hamelers, P.M. Biesheuvel, Nernst-Planck transport theory for (reverse) electrodialysis: I. Effect of co-ion transport through the membranes, J. Memb. Sci. 510 (2016) 370–381. doi:10.1016/j.memsci.2016.03.012.

[22] R. Ortiz-imedio, L. Gomez-coma, M. Fallanza, A. Ortiz, R. Ibañez, I. Ortiz, Comparative performance of Salinity Gradient Power-Reverse Electrodialysis under different operating conditions, Desalination. 457 (2019) 8–21. doi:10.1016/j.desal.2019.01.005.

[23] J.G. Hong, W. Zhang, J. Luo, Y. Chen, Modeling of power generation from the mixing of simulated saline and freshwater with a reverse electrodialysis system: The effect of monovalent and multivalent ions, Appl. Energy. 110 (2013) 244–251. doi:10.1016/j.apenergy.2013.04.015.

[24] J.G. Hong, W. Zhang, J. Luo, Y. Chen, Corrigendum to “Modeling of power generation from the mixing of simulated saline and freshwater with a reverse electrodialysis system: The effect of monovalent and multivalent ions” [Appl. Energy 110 (2013) 244–251], Appl. Energy. 129 (2014) 398–399. doi:10.1016/j.apenergy.2014.05.051.

[25] A.H. Galama, N.A. Hoog, D.R. Yntema, Method for determining ion exchange membrane resistance for electrodialysis systems, Desalination. 380 (2016) 1–11. doi:10.1016/j.desal.2015.11.018.

[26] A.A. Moya, Electrochemical Impedance of Ion-Exchange Membranes with Interfacial Charge Transfer Resistances, J. Phys. Chem. C. 120 (2016) 6543–6552. doi:10.1021/acs.jpcc.5b12087.

[27] P.K. Sow, D. Parvatalu, A. Bhardwaj, B.N. Prabhu, A.N. Bhaskarwar, A. Shukla, Impedance spectroscopic determination of effect of temperature on the transport resistances of an electro-electrodialysis cell used for concentration of hydriodic acid, J. Appl. Electrochem. 43 (2013) 31–41. doi:10.1007/s10800-012-0500-7.

[28] F.Q. Mir, A. Shukla, Sharp rise in resistance of ion exchange membranes in low concentration NaCl solution, J. Taiwan Inst. Chem. Eng. 72 (2017) 134–141. doi:10.1016/j.jtice.2017.01.019.

[29] D.R. Díaz, F.J. Carmona, L. Palacio, N.A. Ochoa, A. Hernández, P. Prádanos, Impedance spectroscopy and membrane potential analysis of microfiltration membranes. The influence of surface fractality, Chem. Eng. Sci., 178 (2018) 27–38. doi:10.1016/j.ces.2017.12.027.

[30] S. Zhu, R.S. Kingsbury, D.F. Call, O. Coronell, Impact of solution composition on the resistance of ion exchange membranes, J. Memb. Sci. 554 (2018) 39–47. doi:10.1016/j.memsci.2018.02.050.

[31] E. Fontananova, E. Curcio, G. Di Profio, A.H. Avci, R.A. Tufa, Reverse Electrodialysis for energy production from natural river water and seawater, Energy. 165 (2018) 512–521. doi:10.1016/j.energy.2018.09.111.

[32] J. Veerman, M. Saakes, S.J. Metz, G.J. Harmsen, Reverse electrodialysis: Performance of a stack with 50 cells on the mixing of sea and river water, J. Memb. Sci. 327 (2009) 136–144. doi:10.1016/j.memsci.2008.11.015.

Highlights

- Modeling the effect of divalent ions on Reverse Electrodialysis performance
- Influence of divalent ions on cation and anion exchange membrane resistances
- Assessment of real water stream ion concentrations for SGE recovery
- Power reduction of 16.3 % in real scenarios in comparison with pure NaCl solutions